Dielectric properties of doped silicon carbide powder by thermal diffusion

SU Xiao-lei(苏晓磊), LI Zhi-min(李智敏), LUO Fa(罗 发), WANG Xiao-yan(王晓艳),
ZHU Dong-mei(朱冬梅), ZHOU Wan-cheng(周万城)

State Key Laboratory of Solidification Processing, Northwestern Polytechnical University, Xi'an 710072, China

Abstract: The doped SiC powders were prepared by the thermal diffusion process in nitrogen atmosphere at 2 000 ℃. Graphite film with holes was used as the protective mask. The dielectric properties of the prepared SiC powders at high frequencies were investigated. The complex permittivity of the undoped and doped SiC powders was measured within the microwave frequency range from 8.2 to 12.4 GHz. The XRD patterns show that before and after heat treatment no new phase appears in the samples of undoped and nitrogen-doped, however, in the aluminum-doped sample the AlN phase appears. At the same time the Raman spectra indicate that after doping the aluminum and nitrogen atoms affect the bond of silicon and carbon. The dielectric real part (ε') and imaginary part (ε'') of the nitrogen-doped sample are higher than those of the other samples. The reason is that in the nitrogen-doped the N atom substitutes the C position of SiC crystal and induces more carriers and in the nitrogen and aluminum-doped the concentration of carriers and the effect of dielectric relaxation will decrease because of the aluminum and nitrogen contrary dopants.

Key words: silicon carbide; dielectric properties; thermal diffusion

1 Introduction

Silicon carbide (SiC) electronic devices and circuits are presently being developed for use in high-frequency, high temperature, high-power, and/or high-radiation conditions[1]. In recent years, as more and more tools taking advantages of microwave come into use, such as mobile telephones, microwave ovens, serious problems on the electromagnetic compatibility and radioprotection have received much attention[2].

Presently, in SiC technology, the silicon carbide powders were prepared by microwave, chemical vapor deposition (CVD), laser- or plasma-driven chemical vapor deposition, sol-gel and carbothermal reduction methods[3−5]. As is well known, doped SiC is realized by ion implantation, diffusion or in-situ doping epitaxial growth and nitrogen (N) and aluminum (Al) are major impurities in the n-type and p-type doping of SiC. ZHAO et al[6] have prepared the nitrogen-doped nano SiC powders and compared their dielectric properties with those of nano pure SiC powder prepared by CVD. SUN et al[7] have prepared the SiC/Al/N by the sol-gel and carbothermal reduction and compared the dielectric

constant of SiC/Al /N nano powders and that of pure SiC nanopowders, respectively. Till now, a little work has been reported on dielectric properties of aluminum-doped SiC in the microwave frequency range by the thermal diffusion processing. Because the thermal diffusion processing is simpler than the other method, it decreases the cost of doped SiC powder possibly.

In this study, the crystal phase and Raman spectra of doped SiC powder by thermal diffusion were analyzed. The complex permittivity of prepared powders was discussed firstly.

2 Experimental

The silicon carbide powder (99.9%, 75 μm, Zhengzhou Dongsheng Abrasives Co Ltd) and aluminum powder were used as the original material and the doping source, respectively. Graphite film with holes was used as the protective mask. The design of crucible is shown in Fig.1. The experimental condition is listed in Table1. Aluminum diffusion was carried out in nitrogen atmosphere, using graphite heating with water-cooled walls. The powders were treated at 2 000 ℃ for 30 min. Because the melting point of aluminum is 660 ℃, at the

high temperature the vapour of aluminum enters the SiC powder through the graphite film with holes.

The powders obtained were washed by hydrochloric acid (HCl) for removing possible aluminum films deposited on the SiC powders surfaces. The crystalline phase of samples was analyzed by the X-ray diffraction(XRD, X'Pert PRO MPD, Cu K_α) and the highly pure Si (99.99%) was used as an external standard. Raman spectroscopic measurements were performed on a Renishow Invia spectrometer for the change of the crystalline phases with the dopant of Al, using the 514.5 nm line of an Ar$^+$ laser as excitation source.
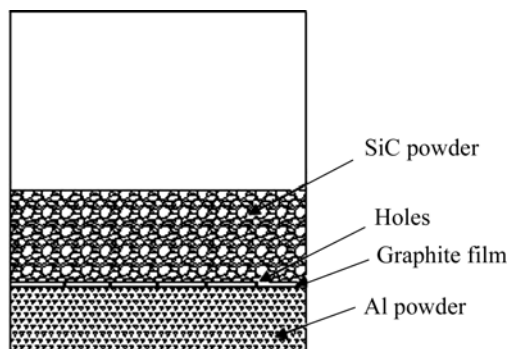

Fig.1 Schematic diagram of crucible design

Table 1 Samples with different conditions

Sample No.	Atmosphere	Temperature/℃	Condition
S_0	Raw material		Undoped
S_1	Vacuum	2 000	Undoped
S_2	Nitrogen	2 000	Undoped
S_3	Nitrogen	2 000	Aluminum-doped

The samples for dielectric parameter measurements were prepared by blending the synthesized powders with paraffin wax in a mass ratio of 7:3, and then molded into 10.16 mm × 22.83 mm × 3 mm flange ring. Commercially available paraffin wax was used. The dielectric parameters were carried out by a network analyzer (HP 8510B) in the frequency range of 8.2−12.4 GHz.

3 Results and discussion

3.1 Phase structure of prepared powders

The XRD patterns of the samples obtained by thermal diffusion process are shown in Fig.2. It can be seen that the dominating phase is the 6H-SiC. No new phase is found both in undoped SiC powders after heat treatment in different atmospheres at 2 000 ℃. However, in the aluminum-doped SiC powder the AlN phase appears.
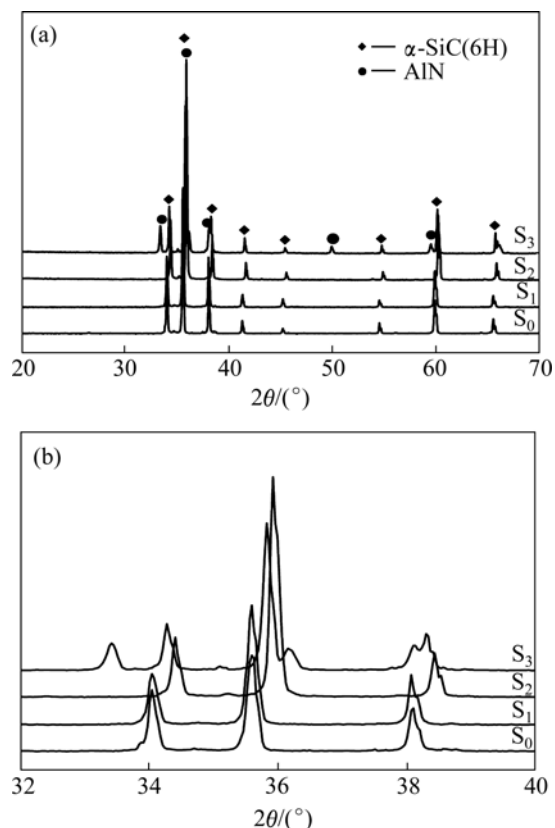

Fig.2 XRD patterns of prepared SiC powders: (a) Original plot; (b) Same data as (a) but with expanding horizontal scale

In the undoped samples the peaks (such as 34.1°, 35.7° and 38.1°, as shown in Fig.2(b)) of SiC phase before and after heat treatment at 2 000 ℃ have no deviation. However, the above peaks of SiC phase shift to higher θ-values in the nitrogen atmosphere, as shown in Fig.2. It indicates that simple heat treatment at 2 000 ℃ changes crystal lattice constant of undoped samples. This is because the N atom enters the SiC crystal and substitutes the position C position. The N atom radius (0.075 nm) is less than that of C atom (0.091 nm), which leads the lattice constant to decrease. In the aluminum-doped sample (S_3) the AlN phase appears and the above peaks of SiC phase shift to higher θ-values. However, the offset of S_3 is smaller than S_2. Those indicate that the offset decreases because of the dopant of Al atom. This is because the Al atoms enter the SiC crystal and substitute the position Si positions. The N atom radius (0.146 nm) is less than that of Al atom (0.182 nm), which leads the lattice constant to decrease.

3.2 Raman spectra

Fig.3 shows the Raman spectra of samples S_0, S_1, S_2 and S_3 in 300−1 400 cm^{-1} region. All of them show the sharply characteristic peaks of 6H-SiC[8−10]. For the S_0, the 6H polytype presents transverse optical FTO(E_2) mode at 766 cm^{-1}, an LO mode at 969 cm^{-1} and Raman

forbidden TO(A_1) mode at 787 cm^{-1}. After 2 000 ℃ treatment in the S$_1$, the bands at 766 cm^{-1} (TO), 787 cm^{-1} (TO) and 969 cm^{-1}(LO) do not change. However, in the S$_2$ and S$_3$, the band shifts to the wavenumber at 770, 785 and 970 cm^{-1} and 770,785 and 969, respectively. The FWHM of the LO band becomes broader and the relative intensities of the Raman spectra are weaker than those of the undoped samples. There are several causes for the shift of the phonon Raman bands relative to those of perfect crystals: 1) strain, 2) phonon confinement, 3) defect or impurity-induced change in the force constants, and 4) defect-induced change in the long-range polarization field[11]. In the S$_2$, the N atom radius is 0.075 nm, which is very close to the Si atom radius (0.091 nm), as the mass of atom is, and the binding energy of N on the site of C of SiC lattice is smaller (1.93 eV)[12]. It is possible that the N atom can substitute the C site on the SiC lattice in the diffusion process, and the resultant solid solution of N/SiC increase the carrier concentration of hole, which makes the band at 969 cm^{-1} weaker and shift to higher wavenumber (970 cm^{-1})[13]. The weakness and high shift of LO band indicates more carriers via LO-phonon-plasmon-coupled mode (LOPC mode) analysis[14−15]. In the S$_3$, though the FWHM of the LO band became broader and the relative intensities of the Raman spectra are weaker than those of the undoped samples, the LO band have no change. So according to the LOPC mode the total carriers have no increase because of the contrary dopants.
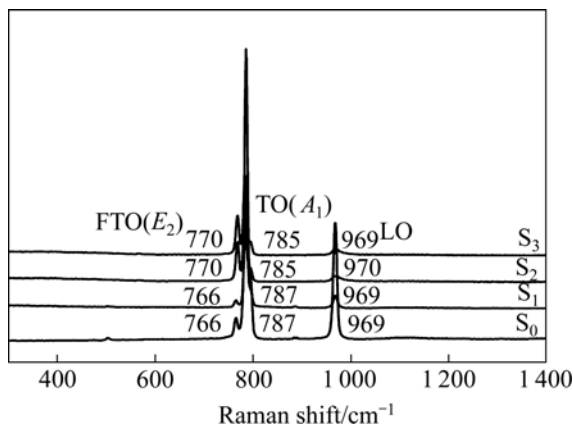

Fig.3 Raman spectra of prepared SiC powders

3.3 Dielectric properties

Fig.4 shows the dielectric real part (ε') and imaginary part (ε'') of all the samples at the microwave frequency range from 8.2 to 12.4 GHz at room temperature. Fig.4(a) shows that the ε' (14.5−13.0) of dielectric properties of the S$_1$ with simply heat treated at 2 000 ℃ are lower than those (18−15) of the S$_0$. The reason is that the impurities resulting from SiC starting

powders are removed and some defects disappear during the high temperature treatment. S$_0$ the total drift mobility of carriers reduce and the ε' and ε'' of the S$_1$ will be lower than those of the S$_0$.
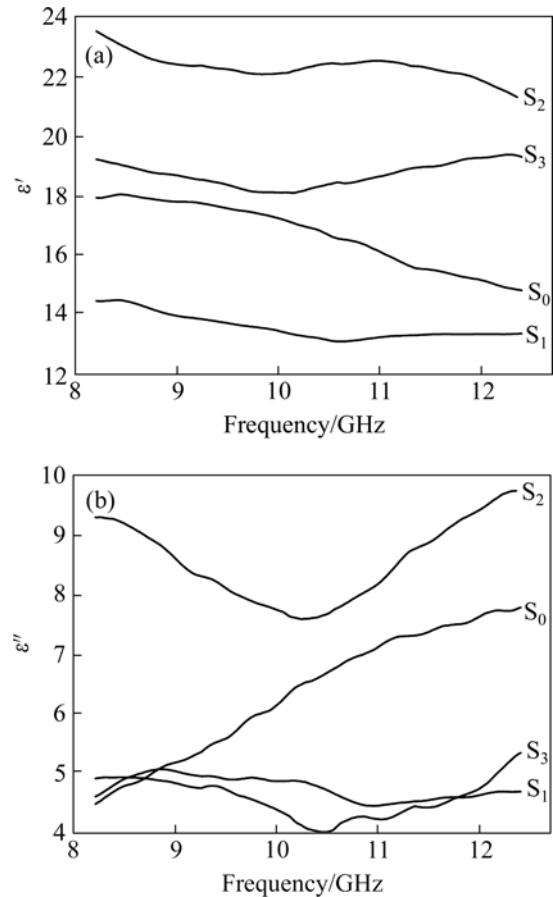

Fig.4 Dielectric real part (a) and imaginary part (b) of prepared SiC powders

In the S$_2$, the N atoms enter the crystal and substitute for the C atoms as a solid solution and N could exist in a nonparamagnetic trivalent form (N(Si)$_3$)[6]. So beside the native defects, the substation induces more defects and unpaired electrons. The charged defects and quasi-free electrons would move in response to the electric field, and diffusion or polarization current results from the field propagation. The charged defects and unpaired electrons in the undoped samples much less than those of the S$_2$. This is the main reason why dielectric real part (ε'=23.8−21.4) and imaginary part (ε''=9.8−7.6) of the S$_2$ are much higher than those of the other samples. Fig.4 shows that dielectric real part (ε') and imaginary part (ε'') of the S$_3$ are 19.1−18.1 and 5.0−4.5, respectively. This is because of two reasons: 1) N and Al atoms enter the SiC crystal at the same time and substitute for the C and Si positions of SiC crystal. The mass defects decrease. 2) The AlN phase has formed in the treatment and the dielectric real part (ε') and imaginary part (ε'') of AlN phase is low ($\varepsilon' \approx 8.1$, $\varepsilon'' \approx 1$).

4 Conclusions

The doped powders were prepared by the thermal diffusion process in nitrogen atmosphere at 2 000 ℃. Graphite film with holes was used as the protective mask. The complex permittivity of the undoped and doped SiC powders was measured within the microwave frequency range from 8.2 to 12.4 GHz. The dielectric real part (ε') and imaginary part (ε'') of the nitrogen-doped sample are higher than those of the other samples. This is because that in the nitrogen-doped sample the N atoms substitute for the C positions of SiC crystal and induce more carriers. In both the nitrogen and aluminum-doped samples the concentrations of carriers decrease because of the aluminum and nitrogen contrary dopants, Therefore, the dielectric real part (ε') and imaginary part (ε'') decrease.

References

[1]   IVAOV A I, CHELNOKOV V E. Recent developments in SiC single-crystal electronics[J]. Semicond Sci Technol, 1992, 7: 863−880.

[2]   ZHANG Bo, LI Jian-bao, SUN Jing-jing, ZHANG Shu-xia, ZHAI Hua-zhang, DU Zheng-wei. Dielectric and infrared properties of silicon carbide nanopowders[J]. J Eur Ceram Soc, 2002, 22: 93−99.

[3]   WANG Xiang-dong, QIAO Guan-jun, JIN Zhi-hao. Preparation of SiC/BN nanocomposite powders by chemical processing[J]. Mater Lett, 2004, 58: 1419−1423.

[4]   DAI Xue-gang, ZHEN Guo-liang, RONG Jing-long, WANG Jian-guo, ZHANG Qi-xiong. Preparation of SiC ultrafine powder by plasma technique[J]. Engineering Chemistry & Metallurgy, 1996, 17(4): 310−315. (in Chinese)

[5]   TIAN Jie-mo, LI Jin-wang, DONG Li-min. Synthesis of SiC precursor by sol-gel process[J]. Journal of Inorganic Materials, 1999, 14(2): 297−301. (in Chinese)

[6]   ZHAO Dong-lin, ZHAO Hong-sheng, ZHOU Wan-cheng. Dielectric properties of nano Si/C/N composite powder and nano SiC powder at high frequencies[J]. Physica E, 2001, 9: 679−685.

[7]   SUN Jing-jing, LI Jian-bao, SUN Ge-liang, ZHANG Bo, ZHANG Shu-xia, ZHAI Hua-zhang. Dielectric and infrared properties of silicon carbide nanopowders[J]. Ceram Int, 2002, 28: 741–745.

[8]   WARD Y, YOUNG R J. Application of Raman microscopy to the analysis of silicon carbide monofilaments[J]. J Mater Sci, 2004, 39: 6781–6790.

[9]   MAHER S AMER, LAVANYA DURGAM, MOSTAFA M. Raman mapping of local phases and local stress fields in silicon-silicon carbide composites[J]. Mater Chem Phys, 2006, 98: 410–414.

[10]   MARTIN H P, MÜLLER E, IRMERH G, BABONNEAU F. Crystallisation behaviour and polytype transformation of polymer-derived silicon carbide[J]. J Eur Ceram Soc, 1997, 17: 659−666.

[11]   NAKASHIMA S, MITANI T, SENZAKI J, OKUMURA H. Deep ultraviolet Raman scattering characterization of ion-implanted SiC crystals[J]. J Appl Phys, 2005, 97: 123507−7.

[12]   HEERA V, PANKNIN D, SKORUPA W. P-type doping of SiC by high dose Al implantation: Problems and progress[J]. Appl Surf Sci, 2001, 184: 307−316.

[13]   TAIROV Y M, RESHANOV S A, PARFENOVA I I, YURYEVA E I, IVANOVSKIL. Theoretical studies of vanadium impurity in β-SiC[J]. Mater Sci Forum, 2002, 389-393: 577−580.

[14]   NAKASHIMA S, HARIMA H, CHOYKE W J, MATSUNAMI H, PENSL G. Silicon carbide－A review of fundamental questions and application to current device technology[M]. Berlin: Akademie Verlag, 1997: 39.

[15]   NAKASHIMA S, HARIMA H. Raman investigation of SiC polytypes[J]. Phys Stat Solidi A, 1997, 162: 39−64.

(Edited by YANG You-ping)